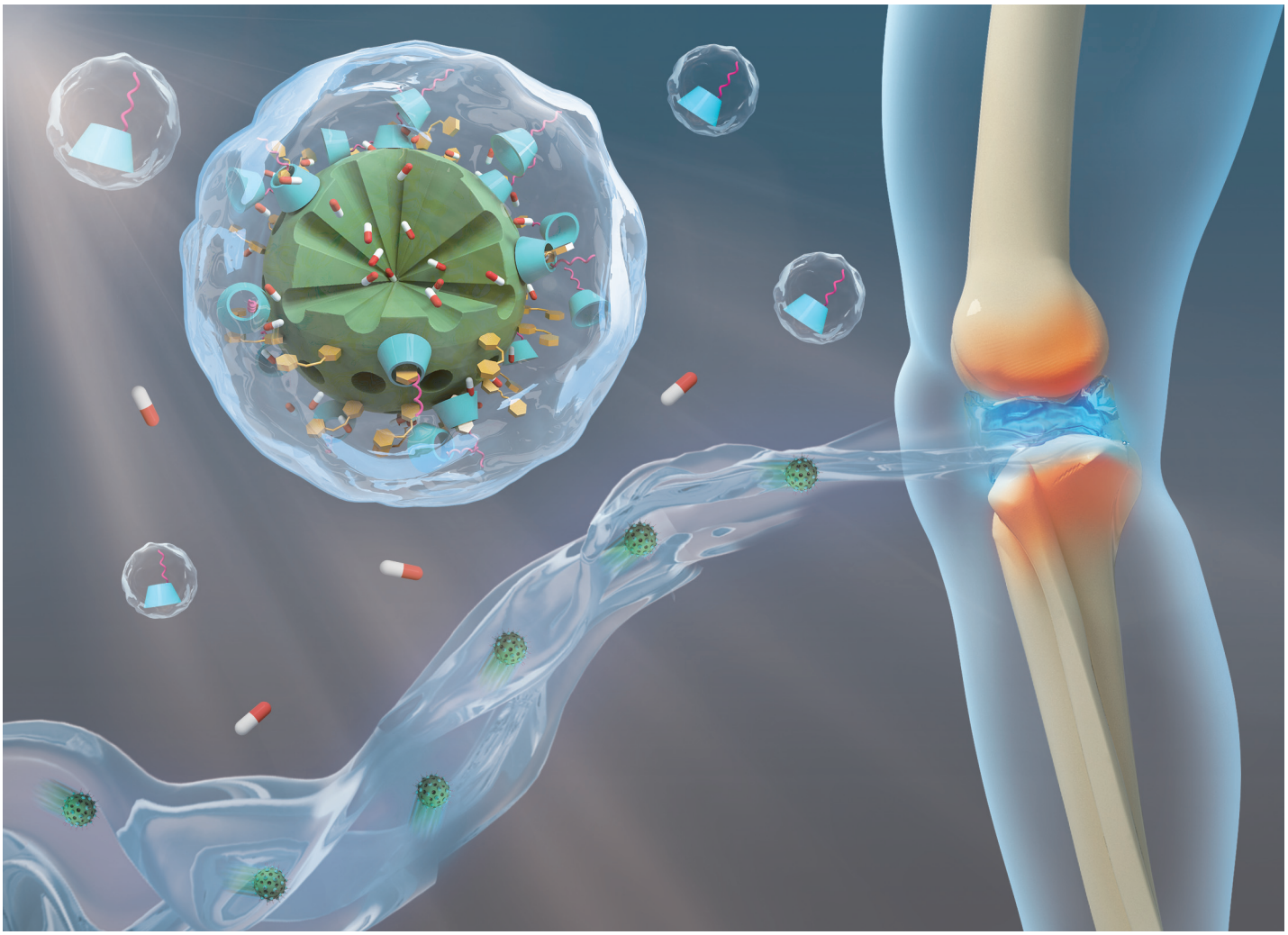

Showcasing research from Professor Hongyu Zhang's laboratory, State Key Laboratory of Tribology, Department of Mechanical Engineering, Tsinghua University, Beijing, China.

Light-responsive dual-functional biodegradable mesoporous silica nanoparticles with drug delivery and lubrication enhancement for the treatment of osteoarthritis

Visible light-responsive biodegradable mesoporous silica nanoparticles featuring both drug delivery and lubrication enhancement were developed for the treatment of osteoarthritis. Visible light could effectively trigger azobenzene isomerization and thus induce drug release after passing through dermal tissue. The hydration layer formed around the phosphorylcholine groups on the surface of the nanoparticles contributed greatly to lubrication enhancement. The synergetic treatment of drug delivery and lubrication enhancement is a promising method for osteoarthritis therapy.

As featured in:

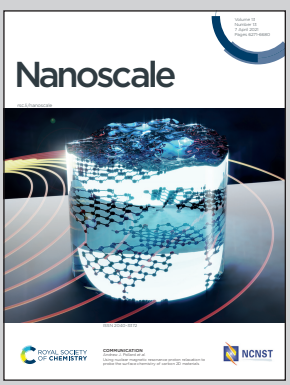

See Bin Feng, Hongyu Zhang *et al.*, *Nanoscale*, 2021, **13**, 6394.

ROYAL SOCIETY OF CHEMISTRY

rsc.li/nanoscale

Registered charity number: 207890

Nanoscale

ROYAL SOCIETY OF CHEMISTRY

COMMUNICATION

View Article Online
View Journal | View Issue

Cite this: *Nanoscale*, 2021, **13**, 6394

Received 16th December 2020,
Accepted 19th February 2021

DOI: 10.1039/d0nr08887k

rsc.li/nanoscale

Light-responsive dual-functional biodegradable mesoporous silica nanoparticles with drug delivery and lubrication enhancement for the treatment of osteoarthritis†

Weiwei Zhao,[a] Hua Wang,[b] Haimang Wang,[a] Ying Han,[a] Zhibo Zheng,[c] Xudong Liu,[d] Bin Feng*[e] and Hongyu Zhang *[a]

Visible light-responsive dual-functional biodegradable mesoporous silica nanoparticles with drug delivery and lubrication enhancement were constructed by supramolecular interaction between azobenzene-modified mesoporous silica nanoparticles (bMSNs-AZO) and β-cyclodextrin-modified poly(2-methacryloyloxyethyl phosphorylcholine) (CD-PMPC). Visible light could effectively trigger azobenzene isomerization and thus induce drug release after passing through the dermal tissue. Additionally, the hydration layer formed by CD-PMPC on the surface of the nanoparticles played an important role in lubrication enhancement, which was beneficial for the treatment of osteoarthritis.

Osteoarthritis (OA) has been regarded as a friction-related disease characterized by both inflammatory irritation and cartilage degradation.[1,2] Improving joint lubrication and alleviating inflammation reaction have been proposed as a promising therapeutic strategy for the treatment of OA.[3–7] However, it is difficult for oral anti-inflammatory drugs to reach the joint and small drug molecules can be quickly removed from the joint cavity, which greatly limits the efficiency of previous treatments. Therefore, encapsulating the drug molecules into a biocompatible nanocarrier is an efficient way to directly deliver the drugs into the joint capsule by local intra-articular injection.

Mesoporous silica nanoparticles (MSNs) have been widely used as drug nanocarriers with large surface area and pore volume, good biocompatibility, and the feasibility for further functionalization.[8–15] An effective control of drug release in space and time using light stimulation can potentially deliver the drugs at targeted tissues and increase local concentration of the encapsulated drug.[16–19] On the other hand, the superlubrication of articular cartilage has been proved to be attributed to hydration lubrication of charged biomacromolecules such as hyaluronic acid, lubricin, collagen and phosphatidylcholine lipid.[20–22] Particularly, the hydration layer surrounding the zwitterionic headgroups in the phosphatidylcholine lipid can bear large joint pressures (4–10 MPa) and thus results in an extremely low friction coefficient (0.001–0.005) at physiological conditions.[23,24] Inspired by this, poly(2-methacryloxyethyl phosphorylcholine) (PMPC), with the same zwitterionic groups as the phosphatidylcholine lipid, has been widely used in surface modification of various substrates to reduce friction coefficient (COF).[25–29] Therefore, the strategy combining light-responsive local drug release and lubrication enhancement is desired to achieve a synergistic effect for the treatment of OA.

In this communication, we reported a visible light-enhanced drug release nanosystem based on the supramolecular interaction between azobenzene-modified biodegradable mesoporous silica nanoparticles (bMSNs-AZO) and β-cyclodextrin-modified poly(2-methacryloyloxyethyl phosphorylcholine) (CD-PMPC). We found that the developed bMSNs-AZO/CD-PMPC nanoparticles could not only improve drug release efficiency upon visible light irradiation but also simultaneously achieve lubrication enhancement. The fabrication approach and proposed mechanism are depicted in Fig. 1. Azobenzene was grafted on the surface of bMSNs to prepare bMSNs-AZO (the synthesis of AZO was shown in Scheme S1†), and CD-PMPC was synthesized *via* free radical polymerization using mono-6-thio-β-CD as the chain transfer reagent and 2,2-azodiisobutyronitrile as the initiator (Scheme S2†). After loading an anti-inflammatory drug diclofenac sodium (DS), CD-PMPC was capped onto the surface of bMSNs-AZO to form

[a]*State Key Laboratory of Tribology, Department of Mechanical Engineering, Tsinghua University, Beijing 100084, China. E-mail: zhanghyu@tsinghua.edu.cn*
[b]*Key Lab of Organic Optoelectronics and Molecular Engineering, Department of Chemistry, Tsinghua University, Beijing 100084, China*
[c]*Department of International Medical Services, Peking Union Medical College Hospital, Chinese Academy of Medical Sciences, Beijing 100730, China*
[d]*Medical Science Research Center, Peking Union Medical College Hospital, Chinese Academy of Medical Sciences, Beijing 100730, China*
[e]*Department of Orthopaedic Surgery, Peking Union Medical College Hospital, Chinese Academy of Medical Sciences, Beijing 100730, China*

†Electronic supplementary information (ESI) available: Material synthesis and characterization, biodegradation tests, drug loading and controlled release experiments, tribological tests, and *in vitro* cytotoxicity studies. See DOI: 10.1039/d0nr08887k

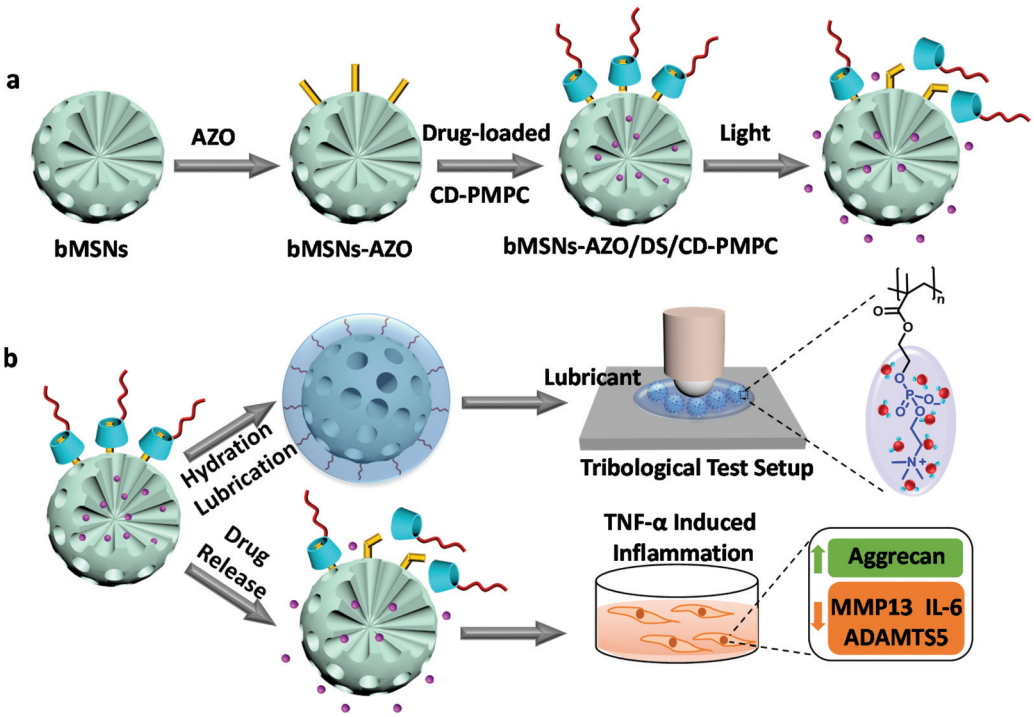

Fig. 1 Schematic illustration of the visible light-responsive dual-functional nanosystem with drug delivery and lubrication enhancement for the treatment of OA. (a) Synthesis of bMSNs nanoparticles and the corresponding modification process. (b) Mechanism of lubrication enhancement and anti-inflammatory properties.

the complex bMSNs-AZO/CD-PMPC based on host–guest interaction, which could block the mesopores and allowed for light-responsive drug release. The controlled release of DS was achieved using a visible light (450 nm), which resulted in the partial *trans*-to-*cis* isomerization of azobenzene and thus dissociation of CD-PMPC from the surface of the nanoparticles. Besides, CD-PMPC endowed the nanoparticles with enhanced lubrication by forming a tenacious hydration layer around the $N^+(CH_3)_3$ and PO_4^- groups in PMPC after light irradiation, which, with a greatly reduced COF value, was beneficial for the treatment of OA. Particularly, the *in vitro* tests showed that light irradiation after passing through the dermal tissue could still stimulate drug release, and the nanoparticles demonstrated excellent anti-inflammatory effect by upregulating anabolic genes and downregulating pro-inflammatory cytokines and catabolic genes. To the best of our knowledge, this study provides for the first time the concept of designing and synthesizing a stimuli-responsive nanosystem based on visible light irradiation for OA therapy.

Biodegradable bMSNs-AZO/CD-PMPC was obtained by dispersing bMSNs-AZO in deionized water and subsequently adding 40 wt% of CD-PMPC to the solution (the characterizations of AZO and CD-PMPC were provided in Fig. S1 and 2†). After blending for 24 h, the modified silica nanoparticles were collected using centrifugation and washed with deionized water to remove excessive CD-PMPC. The morphology, composition, thermodynamics and mesostructure of bMSNs, bMSNs-AZO and bMSNs-AZO/CD-PMPC nanoparticles were characterized by transmission electron microscopy (TEM), X-ray photoelectron spectroscopy (XPS), Fourier transform infrared (FTIR) spectrum, thermogravimetric analysis (TGA), small-angle X-ray diffraction (XRD) spectrum and nitrogen adsorption and desorption, and the results are illustrated in Fig. 2. The TEM images (Fig. 2a–c) show that the diameter of bMSNs before and after the modification is 150 nm with homogeneous radical distribution of internal mesopores. Compared with bMSNs, the channel of the mesopores for bMSNs-AZO/CD-PMPC is blocked by the polymers and becomes unclear, indicating the successful modification of CD-PMPC on the surface. The XPS spectra shown in Fig. 2d and Fig. S3–5† indicate the presence of azobenzene and CD-PMPC groups for bMSNs-AZO/CD-PMPC as the signals of N and P elements have been observed at 402 eV (N 1s), 189 eV (P 2s) and 132 eV (P 2p). The FTIR spectra (Fig. 2e) also confirm the successful surface modification of bMSNs, with the absorption band of benzene ring, C═O and P═O at 1543 cm^{-1}, 1723 cm^{-1} and 1221 cm^{-1}, respectively. The results of TGA (Fig. 2f) show that the weight loss of bMSNs, bMSNs-AZO and bMSNs-AZO/CD-PMPC in the heating process is 10.9%, 14.2% and 37.2%, respectively. Consequently, the contents of AZO and CD-PMPC in bMSNs-AZO/CD-PMPC are calculated to be 3.3% and 23.0%. In addition, the XRD patterns of the nanoparticles (Fig. 2g) show a peak centered at 1.18°, indicating the existence of ordered mesoporous structures in the samples. The mesostructure of the nanoparticles is further investigated by measuring the N_2 adsorption–desorption isotherms, and the surface area,

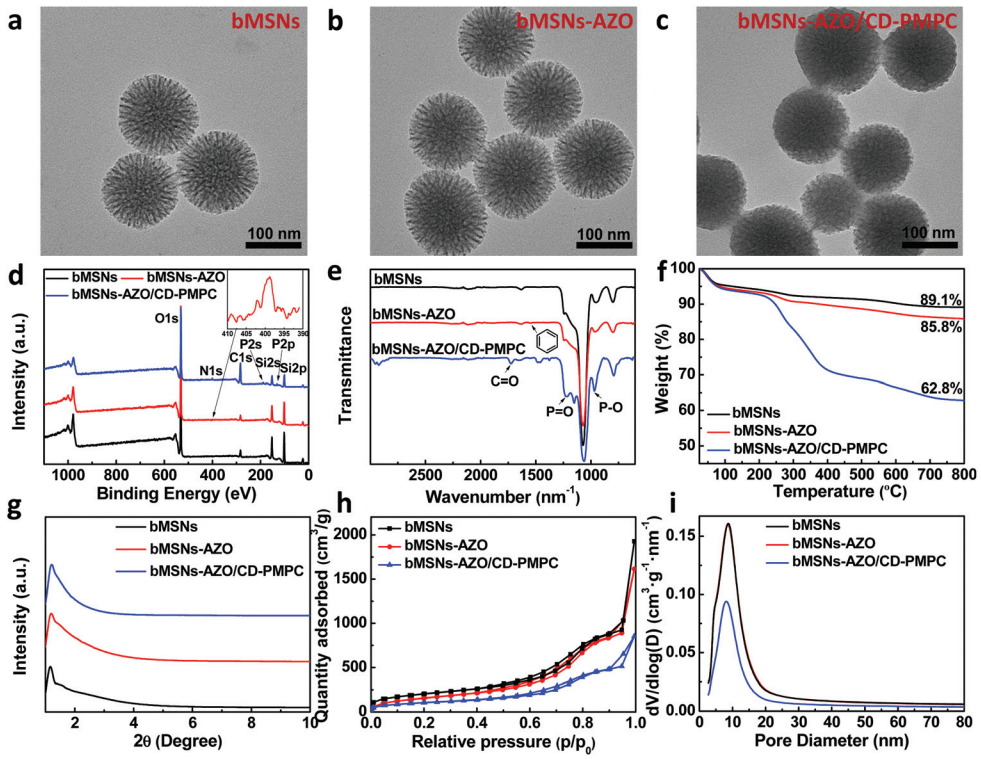

Fig. 2 Characterizations of the nanoparticles. TEM images of bMSNs (a), bMSNs-AZO (b) and bMSNs-AZO/CD-PMPC (c). XPS spectra (d), FTIR spectra (e), TGA curves (f), small-angle XRD patterns (g), N_2 adsorption–desorption isotherms (h) and the pore size distribution (i) of bMSNs, bMSNs-AZO and bMSNs-AZO/CD-PMPC.

pore volume and pore size distribution are illustrated in Fig. 2h, i and Table S1,† based on Brunauer–Emmett–Teller (BET) model and Barrett–Joyner–Halenda (BJH) model. Compared with bMSNs, the modification of CD-PMPC significantly decreases the surface area and pore volume, indicating that the radical channels have been blocked by CD-PMPC. The degradation behavior of the nanoparticles in acidic simulated body fluid is depicted in Fig. S6,† and all the samples are degraded into small fragments in 10 d. The results indicate that bMSNs-AZO/CD-PMPC can be effectively degraded due to the low crosslinking degree of the nanoparticles, making it possible for the utilization in the *in vivo* experiments.

After investigating the mesostructure properties of the nanoparticles, the visible light triggered drug release behavior and lubrication performance were then studied. As upon photoirradiation the azobenzene group can be switched from *trans*-to-*cis* isomerization, the introduction of azobenzene and CD-PMPC to the bMSNs endows the nanosystem with light-responsive property, during which the AZO group experiences configuration conversion and repels itself from the CD cavity. The isomerization of AZO is closely related to light wavelength, and it has been reported that 28% of the azobenzene group isomerization occurs under visible light illumination (λ = 455 nm).[30] Therefore, in the present study a visible light with a wavelength of 450 nm (intensity: 80 mW cm^{-1}) is chosen to stimulate the azobenzene groups for isomerization, considering that the use of visible light can effectively minimize the damage to cells and increase the penetration depth compared with ultraviolet light.[31] Firstly, in order to promote practical application of the nanosystem, the visible light-triggered drug release through a dermal tissue (nude mouse skin) is tested, with the experimental setup shown in Fig. 3a (the UV–vis spectra and ^{1}H NMR spectra of AZO and AZO/β-CD with or without light irradiation are shown in Fig. S7 and 8†). In dark condition (Fig. 3b), the DS release curves from bMSNs, bMSNs-AZO and bMSNs-AZO/CD-PMPC show a very similar trend, where a rapid drug release occurs in the initial stage and afterward gradually reaches a relative plateau stage. The modification of both AZO and AZO/CD-PMPC on the surface of silica nanoparticles leads to a reduction in drug release. The bMSNs-AZO/CD-PMPC nanoparticles modified with different concentrations of CD-PMPC are distinguished by the weight percentage of CD-PMPC in the nanoparticles during the synthesis reaction, *i.e.*, bMSNs-AZO/CD-PMPC 1 (20 wt%), bMSNs-AZO/CD-PMPC 2 (40 wt%) and bMSNs-AZO/CD-PMPC 3 (60 wt%). At 9 h, the release of DS from bMSNs, bMSNs-AZO, bMSNs-AZO/CD-PMPC 1, bMSNs-AZO/CD-PMPC 2 and bMSNs-AZO/CD-PMPC 3 is 78%, 69%, 43%, 31% and 26%, respectively. The sustainable drug release for bMSNs-AZO/CD-PMPC is attributed to the host–guest interaction of AZO and CD-PMPC on the surface of the nanoparticles. It is shown in Fig. 3c that, compared with the result under dark condition (43%), the DS release of bMSNs-AZO/CD-PMPC 1 after direct visible light irradiation for 9 h increases to 62%, whereas it slightly

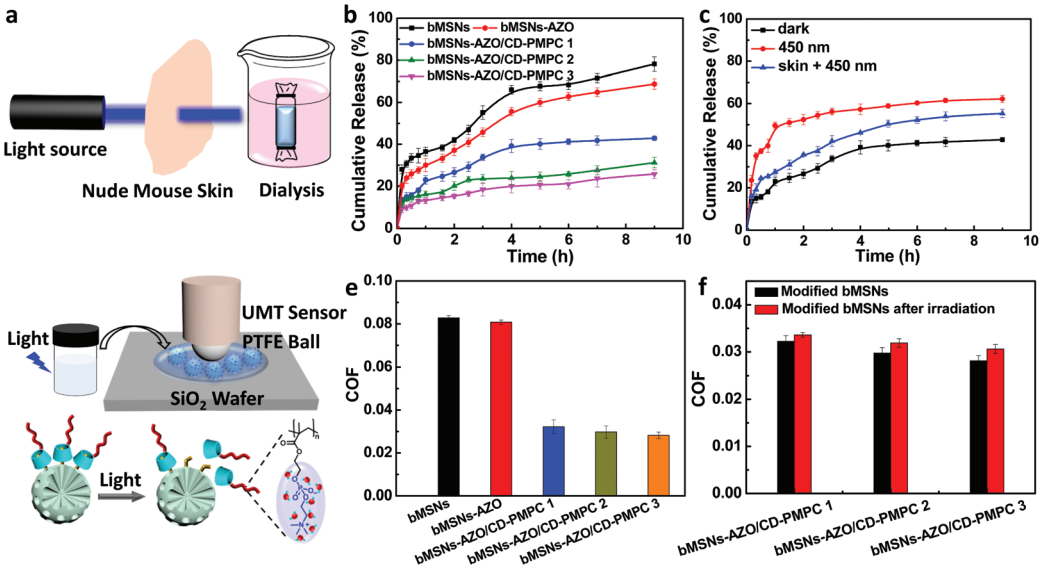

Fig. 3 (a) Schematic illustration of experimental setup showing visible light (450 nm) triggered drug release with a piece of nude mouse skin between the light source and the sample. (b) Release curves of DS from bMSNs, bMSNs-AZO, bMSNs-AZO/CD-PMPC 1, bMSNs-AZO/CD-PMPC 2 and bMSNs-AZO/CD-PMPC 3 under dark conditions. (c) Release curves of DS from bMSNs-AZO/CD-PMPC 1 in the dark, upon visible light irradiation and upon visible light irradiation in the presence of the nude mouse skin. (d) Schematic illustration of tribological test performed using a tribometer and hydration lubrication of bMSNs-AZO/CD-PMPC before and after visible light irradiation. (e) Lubrication property of 2.0 mg mL^{-1} of bMSNs, bMSNs-AZO, bMSNs-AZO/CD-PMPC 1, bMSNs-AZO/CD-PMPC 2 and bMSNs-AZO/CD-PMPC 3 (scanning rate: 2 Hz; loading force: 2 N). (f) Lubrication property of different bMSNs-AZO/CD-PMPC nanoparticles before and after visible light irradiation (scanning rate: 2 Hz, loading force: 2 N; concentration: 2.0 mg mL^{-1}).

decreases to 55% after dermal tissue attenuated irradiation. This indicates that light irradiation induces a faster release of DS (with or without passing through the dermal tissue) owing to the weakened host–guest interaction and correspondingly detachment of CD-PMPC from the surface of the nanoparticles (more detailed DS release curves are shown in Fig. S9–12†). Secondly, the lubrication properties of the nanoparticles are investigated using a universal materials tribometer (UMT) as schematically shown in Fig. 3d. Under dark condition, all the COF values of bMSNs-AZO/CD-PMPC are substantially lower than that of both bMSNs and bMSNs-AZO, with the lubrication performance slightly improved with the increase in the concentration of CD-PMPC (Fig. 3e). The enhanced lubrication is attributed to the hydrated layer formed surrounding the zwitterionic charged groups in CD-PMPC based on hydration lubrication mechanism. The lubrication properties of bMSNs-AZO/CD-PMPC prepared with different CD-PMPC concentrations are also examined at various loading forces, nanoparticle concentrations, and reciprocating frequencies, in which the COF values still remain lower than 0.04 (Fig. S13–15†). Subsequently, the influence of light irradiation on the lubrication performance of the nanoparticles is investigated, and the result is shown in Fig. 3f. Clearly, the visible light triggers AZO isomerization and the partial detachment of CD-PMPC from the surface of the nanoparticles leads to slight increase in the COF value compared with the dark groups. However, all the COF values of bMSNs-AZO/CD-PMPC still remain a low level owing to the excellent lubrication performance of CD-PMPC (more details about the lubrication properties of CD-PMPC, bMSNs and bMSNs-AZO before and after light irradiation are listed in Fig. S16†).

To prove preliminary biomedical application of the developed nanosystem, bMSNs and bMSNs-AZO/CD-PMPC were also applied to living cells, *i.e.* MC3T3-E1 cells, to examine the *in vitro* cytotoxicity and anti-inflammatory function. Clearly, the live/dead staining in Fig. 4a indicate that most of the MC3T3-E1 cells stay alive after incubation for 1 d, 3 d and 5 d, and the cell density increases gradually with the incubation time. Moreover, the *in vitro* cytotoxicity of bMSNs and bMSNs-AZO/CD-PMPC evaluated by Cell Counting Kit-8 (Fig. S17 and 18†) shows that the cell viabilities are higher than 90% for all the incubation times and nanoparticle concentrations tested. These results reveal that cell viability is not affected following incubation with the bMSNs-AZO/CD-PMPC nanoparticles. After that, the protein expression levels of OA-related pro-inflammatory cytokine interleukin-6 (IL-6), matrix metalloproteinases (MMP13), a disintegrin and metalloproteinase with thrombospondin 5 (ADAMTS5) and the anabolic gene aggrecan (Agg) were determined using commercially available enzyme-linked immunosorbent assay (ELISA) kits. Classically, the pathogenesis and development of OA are regulated by many factors. For example, the pro-inflammatory cytokine IL-6 can stimulate the production of reactive oxygen species and alter the metabolism of cells, MMP13 and ADAMTS5 play a vital role in cartilage degradation, while Agg is a major structural component of articular cartilage.[32–35] As shown in

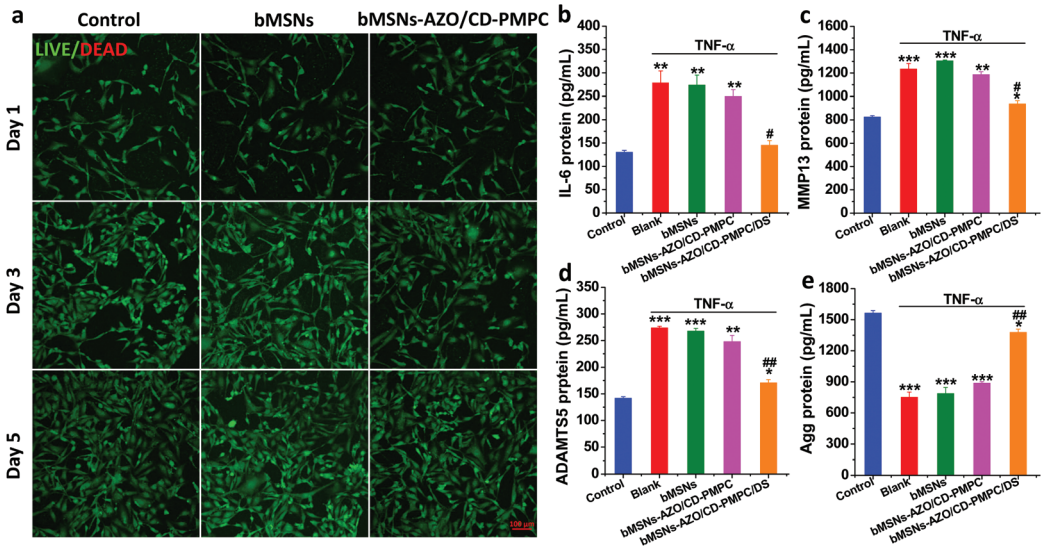

Fig. 4 (a) Confocal images of the MC3T3-E1 cells after incubation with 0.1 mg mL^{-1} of bMSNs or bMSNs-AZO/CD-PMPC for 1, 3 and 5 days, measured by live/dead assay. The protein expression levels of IL-6 (b), MMP13 (c), ADAMTS5 (d) and Agg (e) in the MC3T3-E1 cells treated with 5 nM of TNF-α and then cultured with 0.1 mg mL^{-1} of bMSNs, bMSNs-AZO/CD-PMPC or bMSNs-AZO/CD-PMPC/DS for 12 h, measured by ELISA kits. n = 3, $^{*}p < 0.05$, $^{**}p < 0.01$ and $^{***}p < 0.001$, compared with the control groups; $^{\#}p < 0.05$, $^{\#\#}p < 0.01$ and $^{\#\#\#}p < 0.001$, compared with the blank groups.

Fig. 4b–e, the introduction of tumor necrosis factor-α (TNF-α) simulates the inflammatory condition in the joints, which can significantly upregulate the protein expression of IL-6 (278 pg mL^{-1}, $p < 0.01$), MMP13 (1235 pg mL^{-1}, $p < 0.001$) and ADAMTS5 (274 pg mL^{-1}, $p < 0.001$), and downregulate the production of Agg (752 pg mL^{-1}, $p < 0.001$) compared with the control group. Additionally, the increased protein expression of IL-6, MMP13 and ADAMTS5 and the reduced protein expression of Agg are detected from the groups of bMSNs and bMSNs-AZO/CD-PMPC, which indicates their low anti-inflammatory function. However, the introduction of bMSNs-AZO/CD-PMPC/DS to the MC3T3-E1 cells induces lower protein expression levels of IL-6 (145 pg mL^{-1}, $p < 0.01$), MMP13 (938 pg mL^{-1}, $p < 0.001$) and ADAMTS5 (171 pg mL^{-1}, $p < 0.001$) and higher protein expression level of Agg (1378 pg mL^{-1}, $p < 0.001$) in comparison with that stimulated by TNF-α (more details about bMSNs, bMSNs-AZO/CD-PMPC, bMSNs/DS, bMSNs-AZO/DS or bMSNs-AZO/CD-PMPC/DS treated groups after TNF-α stimulation are shown in Fig. S19†). This indicates that the drug-loaded bMSNs-AZO/CD-PMPC nanoparticles are effective in reducing inflammation while also protecting the cells from degradation.

In this study, visible light-responsive biodegradable mesoporous silica nanoparticles, bMSNs-AZO/CD-PMPC, were successfully constructed for lubrication enhancement and anti-inflammation. By using visible light, partial of the azobenzene groups on the surface of bMSNs experienced isomerization and therefore CD-PMPC was repelled off the nanoparticles, resulting in a sustainable drug release behavior. More importantly, bMSNs-AZO/CD-PMPC effectively improved lubrication performance with or without light irradiation. The lubrication enhancement was attributed to hydration lubrication, where a hydration layer was formed surrounding the zwitterionic groups in CD-PMPC, resulting in a remarkably reduced COF value at the interface. Furthermore, the *in vitro* tests demonstrated that bMSNs-AZO/CD-PMPC possessed good cell compatibility and exhibited promising anti-inflammation function *via* release of a pre-encapsulated drug, revealing its potential application in OA therapy. Combined all the results together, this work was expected to promote the development of a smart nanosystem with stimulus-responsive drug release and lubrication enhancement for the treatment of OA.

Conflicts of interest

The authors declare no competing conflicts of interest.

Acknowledgements

This study was financially supported by National Natural Science Foundation of China (52022043), Tsinghua University–Peking Union Medical College Hospital Initiative Scientific Research Program (20191080593), Precision Medicine Foundation, Tsinghua University, China (10001020107), China Postdoctoral Science Foundation (2019M660620), and Research Fund of State Key Laboratory of Tribology, Tsinghua University, China (SKLT2020C11).

Notes and references

1 D. J. Hunter and S. Bierma-Zeinstra, *Lancet*, 2019, **393**, 1745–1759.

2 J. Knoop, J. Dekker, J. P. Klein, M. Leeden, M. Esch, D. Reiding, R. E. Voorneman, M. Gerritsen, L. D. Roorda, M. P. M. Steultjens and W. F. Lems, *Arthritis Res. Ther.*, 2012, **14**, R212.
3 S. Lue, S. Koppikar, K. Shaikh, D. Mahendira and T. E. Towheed, *Osteoarthritis Cartilage*, 2017, **25**, 1379–1389.
4 R. H. Koh, Y. Jin, J. Kim and N. S. Hwang, *Cells*, 2020, **9**, 419.
5 Y. Zheng, J. Yang, J. Liang, X. Xu, W. Cui, L. Deng and H. Zhang, *Biomacromolecules*, 2019, **20**, 4135–4142.
6 L. Yang, Y. Liu, X. Shou, D. Ni, T. Kong and Y. Zhao, *Nanoscale*, 2020, **12**, 17093–17102.
7 P. Maudens, S. Meyer, C. A. Seemayer, O. Jordan and E. Allémann, *Nanoscale*, 2018, **10**, 1845–1854.
8 A. Watermann and J. Brieger, *Nanomaterials*, 2017, **7**, 189.
9 T. T. H. Thi, V. D. Cao, T. N. Q. Nguyen, D. T. Hoang, V. C. Ngo and D. H. Nguyen, *Mater. Sci. Eng. C*, 2019, **99**, 631–656.
10 J. L. Paris, M. V. Cabañas, M. Manzano and M. Vallet-Regi, *ACS Nano*, 2015, **9**, 11023–11033.
11 J. Zhang, Z. Yuan, Y. Wang, W. Chen, G. Luo, S. Cheng, R. Zhuo and X. Zhang, *J. Am. Chem. Soc.*, 2013, **135**, 5068–5073.
12 Y. Yamauchi, T. Nagaura, A. Ishikawa, T. Chikyow and S. Inoue, *J. Am. Chem. Soc.*, 2008, **130**, 10165–10170.
13 A. Baeza, M. Colilla and M. Vallet-Regí, *Expert Opin. Drug Delivery*, 2015, **12**, 319–337.
14 N. Song and Y. Yang, *Chem. Soc. Rev.*, 2015, **44**, 3474–3504.
15 H. Zhang, W. Cui, X. Qu, H. Wu, L. Qu, X. Zhang, E. Mäkilä, J. Salonen, Y. Zhu, Z. Yang, D. Chen, H. A. Santos, M. Hai and D. A. Weitz, *Proc. Natl. Acad. Sci. U. S. A.*, 2019, **116**, 7744–7749.
16 A. Raza, U. Hayat, T. Rasheed, M. Bilal and H. M. N. Iqbal, *J. Mater. Res. Technol.*, 2019, **8**, 1497–1509.
17 S. Ahmadi, N. Rabiee, M. Bagherzadeh, F. Elmi, Y. Fatahi, F. Farjadian, N. Baheiraei, B. Nasseri, M. Rabiee, N. T. Dastjerd, A. Valibeik, M. Karimi and M. R. Hamblin, *Nano Today*, 2020, **34**, 100914.
18 D. Wang and S. Wu, *Langmuir*, 2016, **32**, 632–636.
19 C.-J. Carling, M. L. Viger, V. A. N. Huu, A. V. Garcia and A. Almutairi, *Chem. Sci.*, 2015, **6**, 335–341.
20 A. Liu, P. Wang, J. Zhang, W. Ye and Q. Wei, *J. Nanosci. Nanotechnol.*, 2019, **19**, 91–97.
21 S. Jahn, J. Seror and J. Klein, *Annu. Rev. Biomed. Eng.*, 2016, **18**, 235–258.
22 J. Seror, Y. Merkher, N. Kampf, L. Collinson, A. J. Day, A. Maroudas and J. Klein, *Biomacromolecules*, 2011, **12**, 3432–3443.
23 J. Klein, *Friction*, 2013, **1**, 1–23.
24 J. Seror, L. Zhu, R. Goldberg, A. J. Day and J. Klein, *Nat. Commun.*, 2015, **6**, 6497.
25 T. Moro, Y. Takatori, K. Ishihara, T. Konno, Y. Takigawa, T. Matsushita, U. Chung, K. Nakamura and H. Kawaguchi, *Nat. Mater.*, 2004, **3**, 829–836.
26 U. Raviv, S. Giasson, N. Kampf, J. F. Gohy, R. Jerome and J. Klein, *Nature*, 2003, **425**, 163–165.
27 M. Chen, W. Briscoe, S. P. Armes and J. Klein, *Science*, 2009, **323**, 1698–1701.
28 M. Kyomoto, T. Moro, Y. Takatori, H. Kawaguchi, K. Nakamura and K. Ishihara, *Biomaterials*, 2010, **31**, 1017–1024.
29 Y. Wang, Y. Sun, Y. Gu and H. Zhang, *Adv. Mater. Interfaces*, 2019, **6**, 1900180.
30 P. Arya, J. Jelken, N. Lomadze, S. Santera and M. Bekir, *J. Chem. Phys.*, 2020, **152**, 024904.
31 A. Mueller, B. Bondurant and D. F. O'Brien, *Macromolecules*, 2000, **33**, 4799–4804.
32 M. Kapoor, J. Martel-Pelletier, D. Lajeunesse, J.-P. Pelletier and H. Fahmi, *Nat. Rev. Rheumatol.*, 2011, **7**, 33–42.
33 P. J. Roughley and J. S. Mort, *J. Exp. Orthop.*, 2014, **1**, 8.
34 M. F. Leeman, S. Curran and G. I. Murray, *J. Pathol.*, 2003, **201**, 528–534.
35 H. Stanton, F. M. Rogerson, C. J. East, S. B. Golub, K. E. Lawlor, C. T. Meeker, C. B. Little, K. Last, P. J. Farmer, I. K. Campbell, A. M. Fourie and A. J. Fosang, *Nature*, 2005, **434**, 648–652.